

# The interdependence of the kinematic and intrinsic parameters of a HIT cell: the effect of charge carrier mobility

## Abstract:

This paper discusses the dependence of the kinematic and intrinsic parameters of a silicon heterojunction solar cell, highlighting mobility phenomena.

First, a three-dimensional schematic of a HIT (Heterojunctions with Intrinsic Thin layer) cell is established to highlight mobility phenomena at the texturized hydrogenated indium oxide ( $\text{In}_2\text{O}_3:\text{H}$ ) contact layer and active layers where charge carriers move.

Next, mathematical equations linking the interacting physical parameters are developed, and the numerical resolution of these mathematical equations has led to results.

The discussion of these results is based on charge carrier transport, more specifically the photocurrent densities of free electrons and excitons, and their contribution in terms of the photovoltaic cell's energy production efficiency.

Key words: nuclear and geothermal energy, effect of charge carrier mobility, Heterojunctions with Intrinsic Thin layer

## Introduction:

Apart from nuclear and geothermal energy, the sun is the source of almost all the energy used by mankind for its food, domestic and industrial needs. Every day, the sun's rays provide the Earth with the equivalent of several thousand times humanity's total energy consumption for its current activities. This solar-generated energy is clean and renewable: there is no pollution or toxic waste that can harm the health of living beings and destroy the environment on Earth and in the atmosphere. We can use this free energy thanks to photovoltaic technologies.

Given the usefulness of this enormous source of energy (the Sun), it would be preferable to improve the efficiency of solar cells, hence the interest of this study. At present, photovoltaic technologies seem to be the best placed to transform the sun's energy into electrical energy that can be used on Earth. But despite the fact that they are by far the best placed, their energy production capacities are only at conversion efficiencies of 16 to 17% (on the market) and reach 30% [1,2] in laboratories. Our contribution will focus on the study of how to improve the efficiency of silicon heterojunction (HIT) solar cells by taking into account the presence of excitons.

For several years now, the photovoltaic industry has been making increasing use of semiconductors to manufacture solar cells. Up until now, most of these cells have been made from silicon, so a great deal of research has been carried out into the physical properties of this material, in order to improve the cell design and solar energy production processes [3,4].

Given that authors have already studied these physical phenomena in different fields and under different circumstances, it is necessary to refer to them in order to gain a better understanding of the subject and contextualise it in our field of study.

M. C. Beard et al [5] used a multiple exciton generation process in colloidal silicon nanocrystals to increase the solar conversion efficiency of homojunction photovoltaic cells.

Richard Corkish et al [6] have shown that excitons, although neutral, can participate in the current of photovoltaic devices by diffusing towards the junction where they can be dissociated by the electric

field, using the generalised theory of three-particle transport (electron, hole and exciton) in semiconductors.

P.N. Rao and al [7], thanks to very low electron and hole mobilities ( $\mu_{e,t} < 10^4 \text{ cm}^2 \cdot \text{V}^{-1} \cdot \text{s}^{-1}$ ), compared with homogeneous crystalline silicon, concluded that drift mobilities are limited by the nanoporous geometry, and not by localised states induced by disorder and acting as traps.

H. Hillmer and others [8] have studied the mobility of two-dimensional excitons in GaAs/Ga<sub>1-x</sub>Al<sub>x</sub>As quantum wells. Comparison of experimental results and calculated mobility limits shows that diffusion disorder at the alloy barrier significantly affects exciton mobilities only in narrow GaAs/ Ga<sub>1-x</sub>Al<sub>x</sub>As quantum wells.

R. D. Schaller and others [9], have experimentally demonstrated that by using semiconductor nanocrystals, they can reduce energy losses at the gap to an almost absolute minimum allowed by the conservation of energy by producing several excitons from a single photon. More precisely, by generating seven excitons from one photon with an energy of 7.8 energy gaps, corresponding to just 10% energy loss, whereas under normal conditions (one photon produces one exciton) 90% of the photon's energy would be dissipated in the form of heat. Such high charge carrier efficiencies have the potential to significantly increase the efficiency of photovoltaic cells and can significantly advance solar power generation technologies.

M. Faye et al [10] have developed a numerical model applicable to inorganic semiconductors in the presence of excitons. They showed that the generation of minority carriers (electrons and excitons) depends on the absorption and average temperature associated with the volume coupling coefficient ( $b = 10^{-2} \cdot T_{\text{moy}}^{-2} + 2,5 \cdot 10^{-6} \cdot T_{\text{moy}}^{-0,5} + 1,5 \cdot 10^{-7}$ ) They also showed that absorption can be dominated by electrons ( $f_e = 1$ ) or excitons ( $f_x = 1$ ).

All these authors, in one way or another, have either used mobility phenomena [8,9] or excitons [6-10] to improve the energy production efficiency of the photovoltaic devices or heterostructures studied. This work was made possible by a theoretical study of the notion of free or bound electron-hole pairs, charge carrier interdependence using a multiphonon or intra-band relaxation method, and mathematical modelling solved using a numerical method developed in reference [11].

The properties of silicon depend on intrinsic and extrinsic parameters such as equilibrium concentrations, gap energy, diffusion and carrier mobility, all of which are linked to temperature. Here we define these parameters and their dependence on temperature, which is often obtained empirically. The interaction of these parameters will be described by a colour code that defines a system of two physical phenomena that we will have to explain.

Given that the mobilities are linked to each other via temperature, we will first combine them with temperature to see their effects on photocurrent densities before making them interact with photocurrent densities and internal quantum yields.

Therefore, to better understand the contribution of mobility to the cell's efficiency in producing energy, we need to demonstrate the mobility phenomena in a silicon heterojunction cell.

## 1. Demonstrating mobility phenomena in a silicon heterojunction cell

The texturing operation aims to develop a micrometric relief on the surface, enabling multiple reflections to reduce the cell's reflectivity. This reduction in reflectivity improves the probability of photon absorption at the surface of the silicon heterojunction cell or high efficiency cell (HIT).

Transparent conductive oxide (TCO) thin films such as , ZnO, SnO<sub>2</sub> and (ITO) are technologically important because of their high optical transparency in the visible range, their wide band gap and their

good electrical conductivity. In addition, indium oxide ( $\text{In}_2\text{O}_3$ ) thin films are one of the most important TCO materials [12,13].

Transparent conducting oxides (TCOs) are in fact degenerate semiconductors. In addition, the high gap of TCOs, between 3 and 4 eV [14,15,16], prevents them from absorbing photons with energies lower than the gap, making them transparent to visible and infrared light.

Incorporating hydrogen into zinc oxide ( $\text{ZnO:H}$ ) and indium oxide ( $\text{In}_2\text{O}_3\text{:H}$ ) TCOs is an effective technique for improving charge carrier mobility [17]. It reduces the transparency-conductivity trade-off within thin films [18].

This mobility enhancement in sputtered  $\text{ZnO:H}$  films reaches  $47.1 \text{ cm}^2 \cdot \text{V}^{-1} \cdot \text{s}^{-1}$  for a carrier concentration of  $4.4 \times 10^{19} \text{ cm}^{-3}$  [19]. Mobility values in excess of  $100 \text{ cm}^2 \cdot \text{V}^{-1} \cdot \text{s}^{-1}$  can be achieved with a charge carrier concentration approaching  $10^{20} \text{ cm}^{-3}$  in  $\text{In}_2\text{O}_3\text{:H}$  films [20,21,22].

As a result, materials with higher mobility than tin-doped  $\text{In}_2\text{O}_3$  (Indium Tin Oxide or ITO) are being successfully implemented in silicon (Si) heterojunctions, following the success of  $\text{In}_2\text{O}_3\text{:H}$ . To achieve low parasitic absorption and high conductivity, the top electrode must have a relatively low carrier density, but high mobility. [23,24,25]

$\text{In}_2\text{O}_3\text{:H}$  is a high-mobility TCO material with superior transmittance in the visible and near infrared [18], and excellent thermal and chemical stability for solar cell applications [26,27].

Thus, in our study we can take into account the excitons that can be excited with infrared light using the  $\text{In}_2\text{O}_3\text{:H}$  on solar cells as a front contact. Where light passes through in order to reach the active layers of the photovoltaic cell. In the case of amorphous or crystalline silicon thin-film solar cells, the light-scattering ability of the TCOs comes into play.

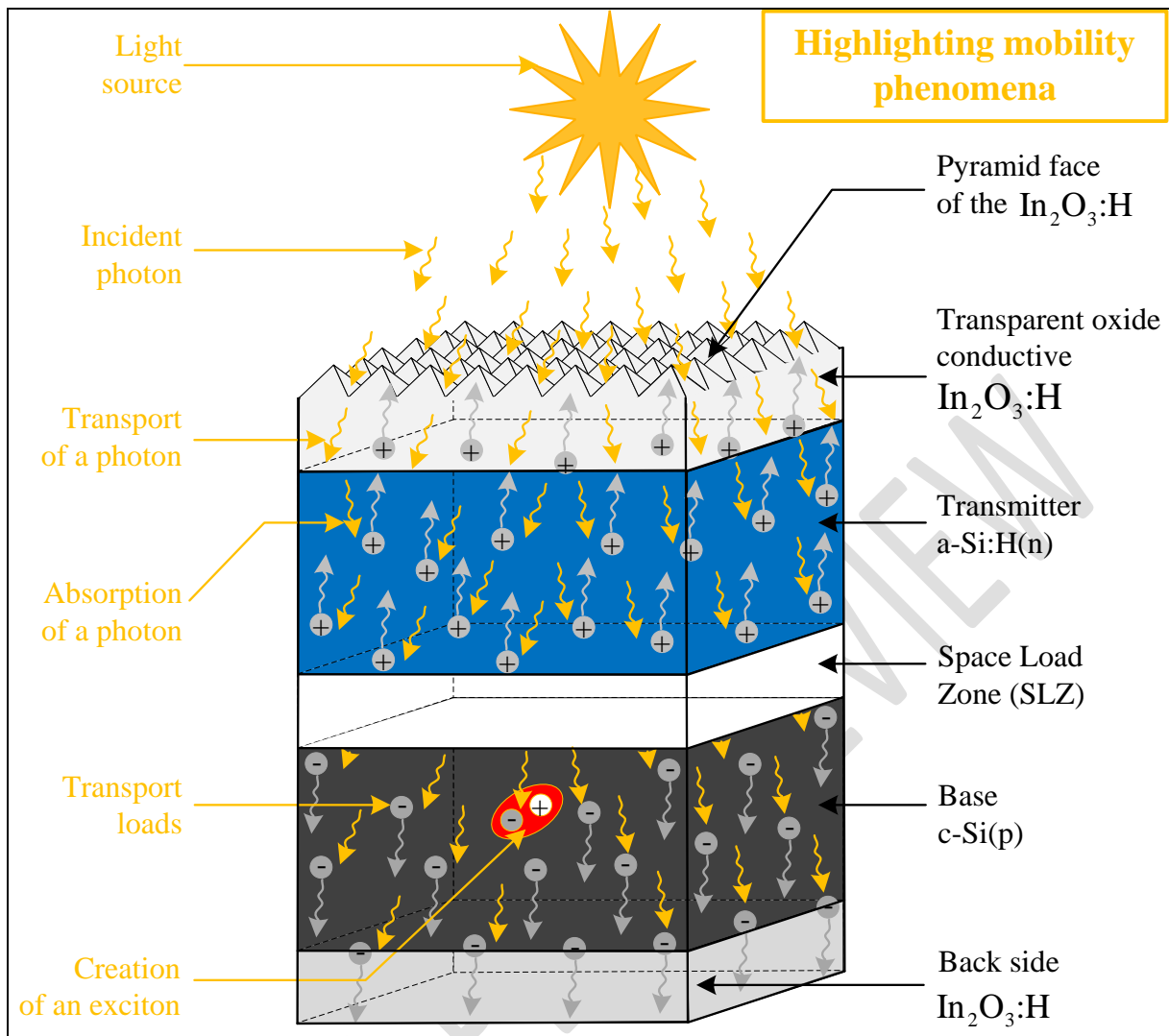


**Figure 1:** Mechanisms of carrier mobility in a sunlit silicon heterojunction cell.

The emitter, doped with donor atoms, has positively-charged holes as minority carriers, while the base, doped with acceptor atoms, has negatively-charged electrons as minority carriers. The emitter and base are the active layers of the HIT cell, where the minority charge carriers are created.

These active layers are separated by a charge-free zone where an electric field prevails due to a potential difference. In the presence of photon energy, the minority charge carriers move through mechanisms of transition from one band to another, separation and propagation towards the receiving electrodes (anode and cathode) with the help of the electric field in the depletion zone.

These propagation or generation mechanisms are more complex with excitons, as the charge carriers in this hydrogenoid complex are linked by an attractive or Coulombic force. Their movement is conditioned by multiphonon and interband relaxations, often leading to annihilation phenomena before being dissociated and recombined.

Since the physical phenomena are interrelated, the electric field of the space charge zone diffuses the minority charge carriers, leading to their mobility. To model these physical phenomena, we have used mathematical equations to express the dependence of kinematic and intrinsic parameters.

## 2. Expressions of some intrinsic and kinematic parameters

### 2.1 Intrinsic parameters

The electronic properties of crystalline silicon depend on intrinsic parameters such as equilibrium free-carrier concentrations, gap energy and the presence of impurities. These parameters are temperature-dependent. Here, we define these parameters and show their dependence on temperature, often obtained empirically.

Equilibrium carrier densities ( $n_{0e}$  for electrons,  $n_{0h}$  for holes) are given by the following expressions:

$$n_{0e}(T) = n_c \times e^{-\frac{(E_c - E_F)}{kT}} \quad \text{and} \quad n_{0h}(T) = n_v \times e^{-\frac{(E_F - E_v)}{kT}}$$

With  $n_c$  and  $n_v$  the respective densities of states of the conduction and valence bands, and  $E_F$  the Fermi energy level.

The values of  $n_c$  and  $n_v$  are often given as  $n_c \approx 3 \times 10^{19} \text{ cm}^{-3}$  and  $n_v \approx 1 \times 10^{19} \text{ cm}^{-3}$  respectively at 300 K [29]. In fact, a parameterization taking into account the evolution of effective masses with temperature between 200 K and 500 K was given by Green [30]:

$$n_c(T) = 3 \times 10^{19} \times \left(\frac{T}{300}\right)^{1.5} \quad \text{and} \quad n_v(T) = 1 \times 10^{19} \times \left(\frac{T}{300}\right)^{1.5}$$

We can base this on the intrinsic density of state, which in addition to being a function of temperature (T), is also expressed as a function of the gap energy ( $E_g$ ), which is an energy difference between the valence band and the conduction band, of respective density of state  $n_v$  and  $n_c$ . Hence the product  $n_{0e} \times n_{0h}$ , which defines the intrinsic carrier density:

$$n_i(T) = \sqrt{n_{0e} \times n_{0h}}$$

Taking the above into account, the intrinsic carrier density is then rewritten as:

$$n_i(T) = (n_c \times n_v)^{0.5} \times e^{-\left(\frac{E_g(T)}{2 \times V_T}\right)}$$

Where A is the thermal potential defined as:

$$V_T = \frac{k_b \times T}{q}$$

And  $E_g$  the temperature-dependent gap energy, described by several empirical models developed since the 60s [31]. The most common model is that given by Varshni (with Thurmond coefficients) [32,33], corroborated more recently by photoluminescence measurements [34], and valid up to temperatures above 750 K:

$$E_g(T) = E_g(0) - \frac{\delta \times T^2}{T - \beta}$$

Gap energy depends on the intrinsic parameters  $\beta$  and  $\delta$  of the material used. For silicon, we obtain a value for  $\beta = 636 \pm 50 \text{ K}$  and a value for  $\delta = 4.73 \times 10^{-4} \text{ eV.K}^{-1}$ .

Intrinsic parameters play a key role in the conversion of photon energy into electrical energy, through the ordered movement of charged electrons, which is facilitated by the crystallographic structure of silicon. Silicon in its intrinsic state, without any external influence, behaves like an insulator and doesn't

allow electrons to move. But in the presence of a few extrinsic parameters: temperature, doping and  $h\nu$ -energy photons, it becomes not only a conductor of energy, but also a producer of electricity.

## 2.2 Kinematic parameters

In addition to intrinsic parameters, there are extrinsic parameters such as doping levels, which give rise to a potential difference  $V_b$  that depends on the thermal potential  $V_T$ , the intrinsic density of state  $n_i$  and the doping levels of acceptors  $N_A$  and donors  $N_D$ .

$$V_b = V_T \times \ln \left( \frac{N_A \times N_D}{n_i^2} \right)$$

This internal potential leads to an electric field  $\vec{E}$ , which allows charge carriers to diffuse into the material.

Since the study focuses on two types of charge carriers, free electrons and excitons, we have defined the diffusion coefficients of free electrons  $D_e$  and excitons  $D_x$  as follows:

$$D_e = V_T \times \left[ 86.5 + 1268 \left( 1 + \frac{N_A}{7.7 \times 10^{18}} \right)^{-0.91} - \left( \frac{1.4 \times 10^{19}}{N_A} \right) \right] \times \left( \frac{T}{300} \right)^2 \quad \text{and} \quad D_x = \frac{300}{T^{0.5}}$$

From the charge carrier diffusion coefficients we deduce the mobility coefficients.

The mobility of free carriers in silicon has been measured mainly by the Hall effect [21] and by high-speed and high-frequency devices [35]. Empirical [36,37,38,39] and analytical formulations have been proposed as a function of doping atom density (As, P or B) and temperature. The most widely used formulation for doping dependence is that of Masetti et al. [39], valid in the following doping density intervals ( $\text{cm}^{-3}$ ):  $[10^{13}, 5 \times 10^{21}]$  and  $[10^{14}, 1.2 \times 10^{21}]$  for phosphorus and boron respectively.

Charge carrier mobility ( $\mu_{e,x}$ ) depends on the material's intrinsic parameters. The latter, together with external parameters [40,41], condition the movement of charge carriers in a photovoltaic cell.

$$\mu_{e,x}(T) = \frac{D_{e,x}}{V_T}$$

This kinematic parameter plays a key role in the dependence of kinematic and intrinsic parameters on solar cell performance.

## 3. Dependence of photocurrent densities on electron and exciton mobilities

Since mobilities are linked to each other via temperature, we'll first combine them with temperature to see their effects on photocurrent densities and internal quantum yields. So, to better understand the effect of temperature on charge carrier mobilities, a study of the influence of temperature is in order.

### 3.1. The effect of temperature on charge carrier mobility

An increase in temperature leads to a decrease in exciton mobility and an increase in electron mobility. The simultaneous variation in carrier mobility as a function of temperature is defined by a color code.

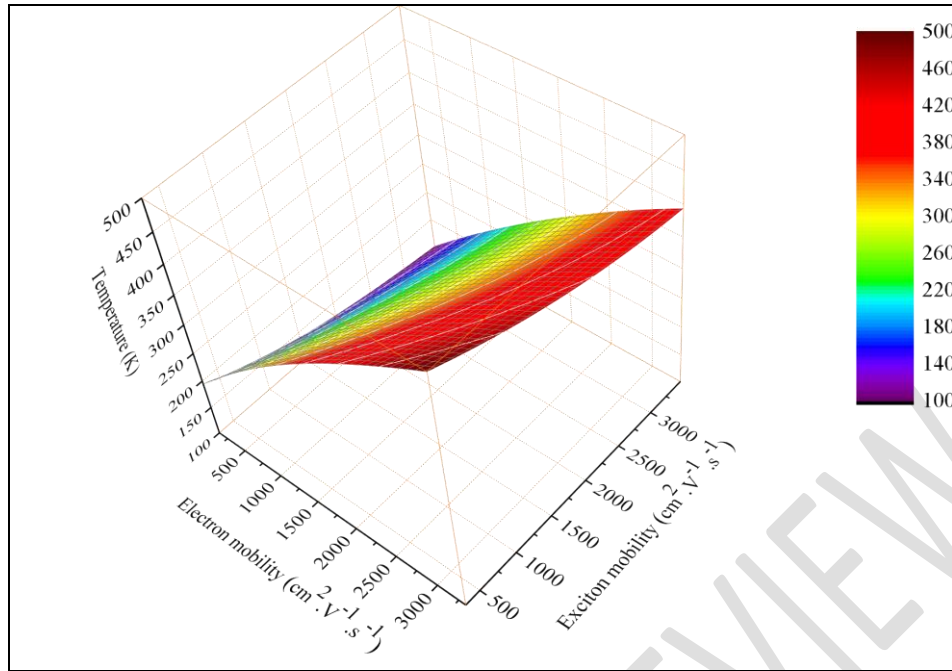


**Figure 2:** The simultaneous influence of temperature on the mobility of free and bound charge carriers (excitons)

The antagonistic phenomena of free electron and exciton mobilities with respect to temperature are observed, and they compensate each other in a balanced way with respect to temperature. Variations in charge carrier mobility are governed by a thermal energy source that enables the cell to conserve photogenerated energy.

### 3.2. The simultaneous effect of temperature and electron mobility on electron photocurrent density

Figure 3 shows the photocurrent density of electrons as a function of temperature and electron mobility.

We obtain low photocurrent densities (below  $6.27 \text{ mA} \cdot \text{cm}^{-2}$ ) at temperatures below 250 K whatever the electron mobility between 250 and  $3500 \text{ cm}^2 \cdot \text{V}^{-1} \cdot \text{s}^{-1}$ . Above a temperature of 250 K, electron photocurrent density increases progressively to  $22.30 \text{ mA} \cdot \text{cm}^{-2}$  for electron mobilities between 1000 and  $2000 \text{ cm}^2 \cdot \text{V}^{-1} \cdot \text{s}^{-1}$ .

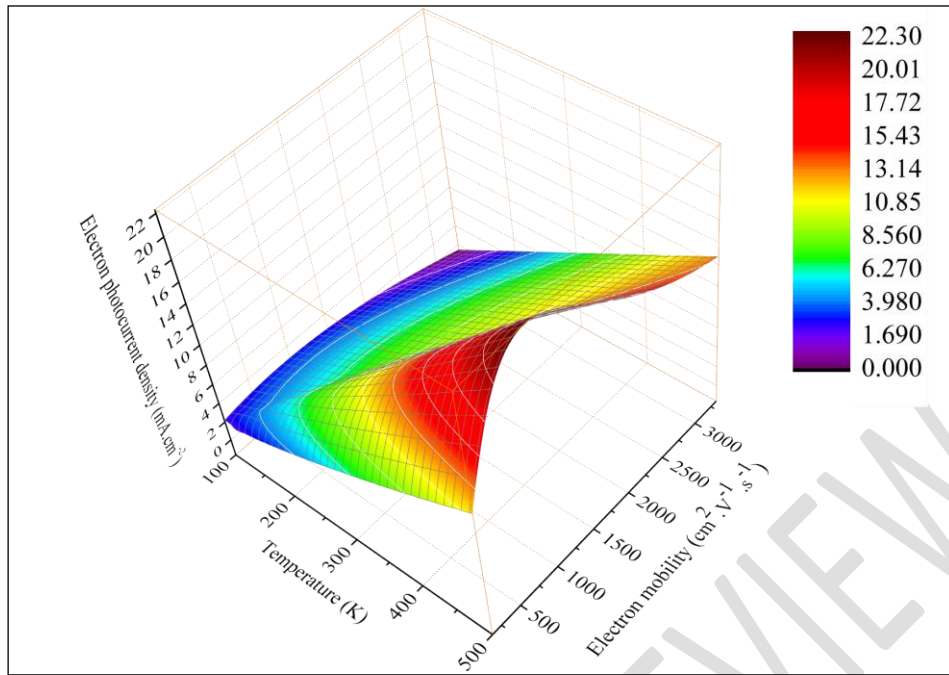


**Figure 3:** Electron photocurrent density as a function of temperature and electron mobility

The excitatory effect of temperature on semiconductor electrons promotes the orderly movement of charge carriers, but not more than the mobility of free electrons. This mobility, although facilitated by temperature, has a more consequential influence on photocurrent density at values around  $1000 \text{ cm}^2 \cdot \text{V}^{-1} \cdot \text{s}^{-1}$  where we obtain the maximum photocurrent density of electrons.

Mobilities below  $500 \text{ cm}^2 \cdot \text{V}^{-1} \cdot \text{s}^{-1}$  coincide with low temperatures, synonymous with inactivation of the cell's electronic structure. Whereas mobilities above  $1500 \text{ cm}^2 \cdot \text{V}^{-1} \cdot \text{s}^{-1}$  coincide with high temperatures, synonymous with disorder in the cell's electronic structure.

As a result, we don't have to grope to see which mobility value is more suitable to get the maximum photogenerated free carriers.

Excitons often behave in the opposite way to free charge carriers in certain physical phenomena. Following on from our work, we have developed a study of the simultaneous effect of temperature and exciton mobility on exciton photocurrent density.

### 3.3 The simultaneous effect of temperature and exciton mobility on exciton photocurrent density

In Figure 4, for exciton mobilities ranging from 250 to  $2500 \text{ cm}^2 \cdot \text{V}^{-1} \cdot \text{s}^{-1}$  and temperatures between 250 K and 500 K, we observe exciton photocurrent densities below  $1.322 \text{ mA} \cdot \text{cm}^{-2}$ . At temperature values below 250 K or very low around 100 K, we observe a slight increase in exciton photocurrent density up to  $1.37 \text{ mA} \cdot \text{cm}^{-2}$  and a maximum peak of  $1.433 \text{ mA} \cdot \text{cm}^{-2}$  at exciton mobilities above  $3000 \text{ cm}^2 \cdot \text{V}^{-1} \cdot \text{s}^{-1}$ .

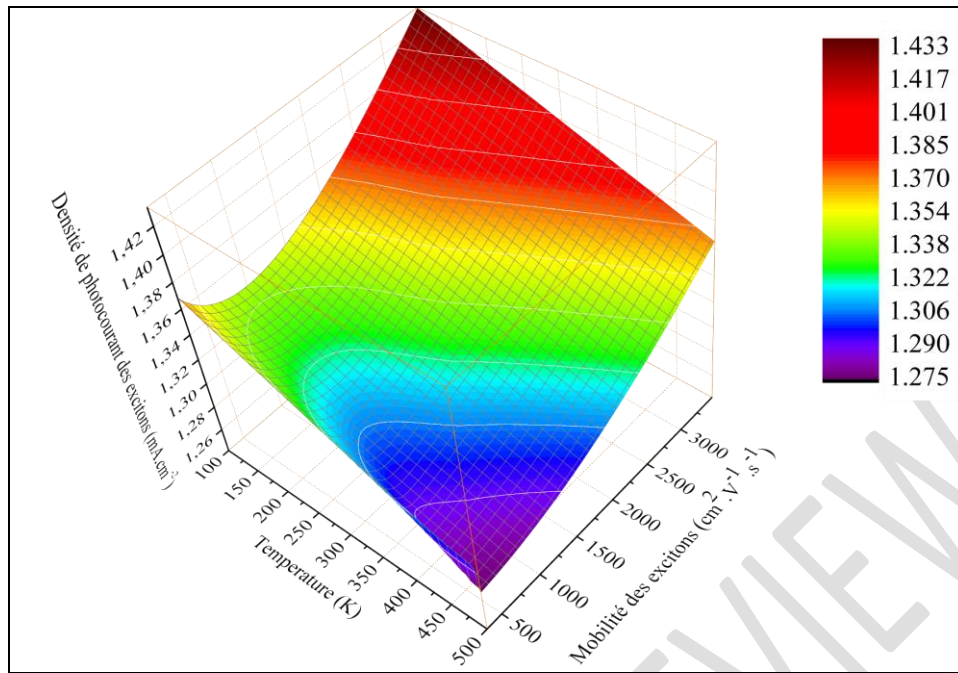


**Figure 4:** Exciton photocurrent density as a function of temperature and exciton mobility

The excitatory effect of temperature on the semiconductor excitons disfavors the ordered movement of excitons, but no more than the mobility of excitons. This mobility, although facilitated by temperature, adversely affects the photocurrent density at values around  $1000 \text{ cm}^2 \cdot \text{V}^{-1} \cdot \text{s}^{-1}$  where we obtain the minimum photocurrent density of excitons. Hence the antagonistic phenomenon of mobility on the photocurrent densities of free electrons and that of excitons.

We're not looking for the maximum number of excitons photogenerated in the cell, but above all the maximum number of charge carriers photogenerated. If we keep temperatures low to obtain the maximum number of photogenerated excitons, we risk a drastic loss of photogenerated free electrons of  $20.0 \text{ mA} \cdot \text{cm}^{-2}$  for a small gain in photogenerated excitons of  $0.079 \text{ mA} \cdot \text{cm}^{-2}$ . This study is therefore designed to obtain the maximum photocurrent density of charge carriers at suitable mobilities.

We will also study the interdependence between photocurrent densities, electron mobilities and exciton mobilities.

### 3.4. The simultaneous effect of electron and exciton mobilities on electron photocurrent density

Figure 5 shows the photocurrent density of electrons as a function of the respective electron and exciton mobilities.

Whatever the mobility value between  $500$  and  $3500 \text{ cm}^2 \cdot \text{V}^{-1} \cdot \text{s}^{-1}$ , the electron photocurrent density exceeds  $8.0 \text{ mA} \cdot \text{cm}^{-2}$  and can approach  $13.0 \text{ mA} \cdot \text{cm}^{-2}$  at exciton mobilities below  $500 \text{ cm}^2 \cdot \text{V}^{-1} \cdot \text{s}^{-1}$ . We also noticed a decrease in electron photocurrent density as exciton mobility increased.

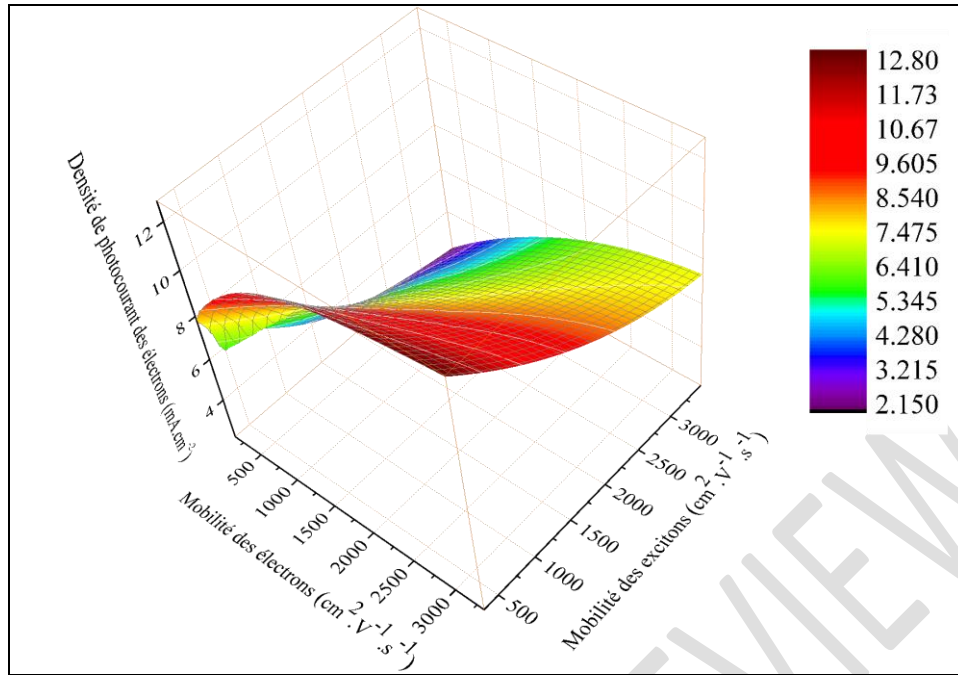


**Figure 5:** Electron photocurrent density as a function of electron and exciton mobility

For charge carrier mobility to be beneficial to electron photocurrent density, free charge carriers must be more mobile and excitons less mobile. High mobility of free electrons enables them to photogenerate as quickly as possible, minimizing recombination. This mobility, facilitated by temperature, is partly due to the electric field in the depletion zone and partly to the photon energy allocated to them by a light source. In addition, high electron mobility is synonymous with energy conservation, as this increasing mobility is due to a source of thermal energy. In addition, this conservation of photon energy must be accompanied by stability of the semiconductor structure. This stability is controlled by the low mobility of the excitons.

As we have seen in Figure 2, the antagonistic character of charge carrier mobilities on electron photocurrent density is observed. In other words, the lowest values of electron photocurrent density are obtained at very low values of electron mobility and very high exciton mobilities. This simultaneous influence of mobilities on electron photocurrent density is balanced. This is not the case for exciton photocurrent density.

### 3.5. The simultaneous effect of electron and exciton mobilities on exciton photocurrent density

Furthermore, we found in Figure 6 that the exciton photocurrent density reaches a maximum peak of  $2.22 \text{ mA} \cdot \text{cm}^{-2}$  with free electron and exciton mobilities below  $1000 \text{ cm}^2 \cdot \text{V}^{-1} \cdot \text{s}^{-1}$ . We also noted a slight increase in photocurrent density, relative to exciton mobility from a value of  $1.27 \text{ mA} \cdot \text{cm}^{-2}$  to a value of  $1.46 \text{ mA} \cdot \text{cm}^{-2}$ .

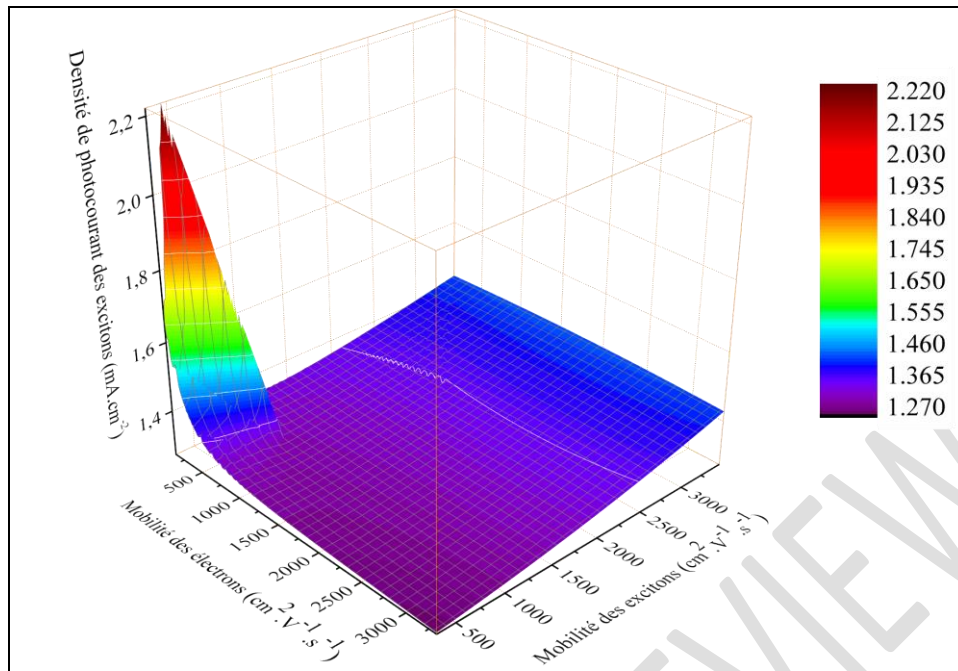


**Figure 6:** Exciton photocurrent density as a function of electron and exciton mobility

When free electrons lose their mobility, they are able to relax to excited levels, contributing a surplus to the excitons already present in the cell. This contribution, shown in Figure 6, is greater than that of the excitons, which increases with their mobility. The excitonic quantities studied therefore provide a surplus of exciton photocurrent densities, acting as energy conservers through a process of intra-band relaxation of free electron-hole pairs. This enables us to conserve some of the photogenerated energy in poor weather conditions. This excitonic phenomenon may also explain the low currents observed in the dark.

It's good to know how and by how much charge carriers are photogenerated. But it's even better to know how much energy photovoltaic cells produce. And the quantum efficiency of charge carriers gives us an insight into this energy contribution. Since we have two types of charge carrier, it's a good idea to study the contribution of each and deduce their utility.

### 3.6. The behavior of the internal quantum yield of charge carriers on the physical parameters studied

Consequently, whatever the temperature or electron mobility, associated with exciton mobility below  $1000 \text{ cm}^2 \cdot \text{V}^{-1} \cdot \text{s}^{-1}$ , we obtain charge carrier internal quantum yields between 50 and 76.8 %. These internal charge carrier quantum yields are shown in Figures 7 and 8.

Whether it's temperature or electron mobility, we obtain better quantum yields than when associating them with low exciton mobilities. We can therefore state that exciton mobility is an excitonic phenomenon that adversely affects charge carrier internal quantum yields, in contrast to free electron mobility, which leads to internal quantum yields in excess of 50 %.

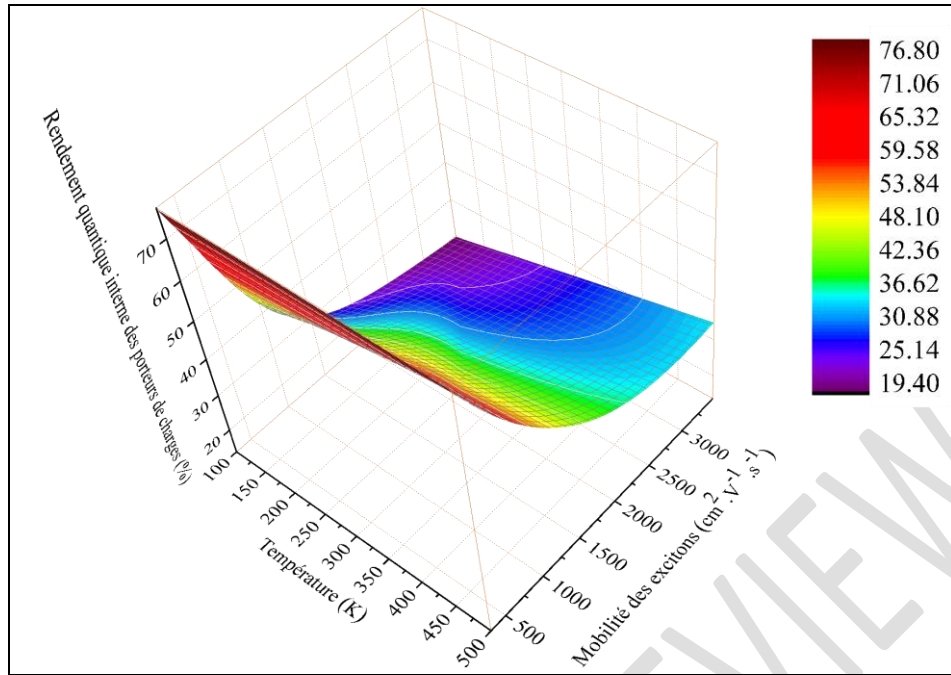


**Figure 7:** Internal quantum yield of charge carriers as a function of temperature and exciton mobility

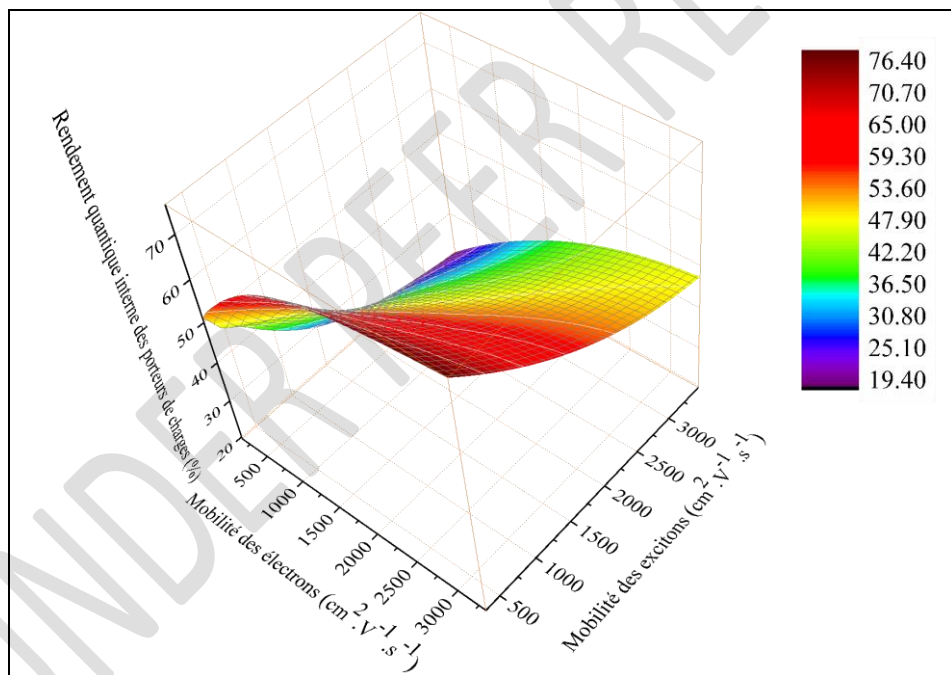


**Figure 8:** The internal quantum yield of charge carriers as a function of electron and exciton mobility.

So we can by making these types of cell avoided having exciton mobility values that exceed 1000 cm<sup>2</sup>·V<sup>-1</sup>·s<sup>-1</sup> to have maximum charge carrier internal quantum efficiency and good photovoltaic energy production from the HIT cell.

### Conclusion:

Variations in charge carrier mobilities are governed by a thermal energy source that enables the cell to conserve the energy photogenerated by free charge carriers and excitons. The excitonic quantities studied not only allow us to have a surplus of exciton photocurrent densities, they also play a role in energy conservation through an intra-band relaxation process of free electron-hole pairs. This enables

us to conserve some of the photogenerated energy in poor weather conditions. This excitonic phenomenon may also explain the low currents observed in the dark.

We're not looking for the maximum number of excitons photogenerated in the cell, but rather the maximum number of charge carriers photogenerated. If we keep temperatures low to obtain the maximum number of photogenerated excitons, we risk a drastic loss of photogenerated free electrons of  $20.0 \text{ mA} \cdot \text{cm}^{-2}$  for a small gain in photogenerated excitons of  $0.079 \text{ mA} \cdot \text{cm}^{-2}$ . So this study is also designed to obtain the maximum photocurrent density of charge carriers at suitable temperatures.

So we can when fabricating these types of cell take into account exciton mobility values around  $1000 \text{ cm}^2 \cdot \text{V}^{-1} \cdot \text{s}^{-1}$  to have internal charge carrier quantum efficiencies approaching 70 % and good photovoltaic energy production from the HIT cell.

Disclaimer (Artificial intelligence)

Option 1:

Author(s) hereby declare that NO generative AI technologies such as Large Language Models (ChatGPT, COPILOT, etc) and text-to-image generators have been used during writing or editing of manuscripts.

Option 2:

Author(s) hereby declare that generative AI technologies such as Large Language Models, etc have been used during writing or editing of manuscripts. This explanation will include the name, version, model, and source of the generative AI technology and as well as all input prompts provided to the generative AI technology

Details of the AI usage are given below:

- 1.
- 2.
- 3.

#### References:

- [1]. O. Palais. Photovoltaic cells: the crystalline silicon industry today and tomorrow. *Mat. and Tech.*, 2009, Vol. 97, N°4, pp 241-245.
- [2]. L. Stoyanov, G. Notton et V. Lazarov. Optimisation of multi-source renewable energy electricity generation systems. *Renewable Energy Review*, 2007, Vol. 10, N°1, pp 1-18.
- [3]. Abdolazadeh Ziabari, A., & Bagheri Khatibani, A. (2017). Optical properties and thermal stability of solar selective absorbers based on Co–Al<sub>2</sub>O<sub>3</sub> cermets. *Chinese Journal of Physics*, 55(3), 876–885.

- [4]. Mirzaei, M., Hasanzadeh, J., & Ziabari, A. A. (2020). Efficiency Enhancement of CZTS Solar Cells Using Al Plasmonic Nanoparticles: The Effect of Size and Period of Nanoparticles. *Journal of Electronic Materials*, 49(12), 7168–7178.
- [5]. M. C. Beard, K. P. Knutsen, P. Yu, J. M. Luther, Q. Song, W. K. Metzger, R. J. Ellingson, and A. J. Nozik. Multiple Exciton Generation in Colloidal Silicon Nanocrystals. *Nano Letters*, 2007, Vol. 7, N°8, pp 2506-2512.
- [6]. R. Corkish, D. S.-P. Chan, and M. A. Green. Excitons in silicon diodes and solar cells : A three-particle theory. *J. Appl. Phys.*, 1996, Vol. 79, N°1, pp 195-203.
- [7]. P. N. Rao, E. A. Schiff, L. Tsybeskov and P. Fauchet. Photocarrier drift-mobility measurements and electron localization in nanoporous silicon. *Chemical Physics*, 2002, Vol. 284, Issues 1-2, pp 129-138.
- [8]. H. Hillmer, A. Forchel, S. Hansmann, M. Morohashi, and E. Lopez. Optical investigations on the mobility of two-dimensional excitons in 1 xx GaAs Ga Al As quantum wells. *The American Physical Society*, 1989, Vol. 39, N°15, pp 10901-10912.
- [9]. R. D. Schaller, M. Sykora, J. M. Pietryga, and V. I. Klimov. Seven Excitons at a Cost of One : Redefining the Limits for Conversion Efficiency of Photons into Charge Carriers. *Nano Letters*, 2006, Vol. 6, N°3, pp 424-429.
- [10]. M. Faye, M. Niane, S. Ndiaye, O. Ngom, C. Mbow, B. Ba. Numerical Modeling of Effects of Excitons on Photoelectric Properties of Cells. *Journal of Scientific and Engineering Research*, 2019, Vol. 6, N°6, pp 138-146.
- [11]. O. Ngom, M. Faye, M. Mbaye, C. Mbow and B. Ba. Numerical Study of the Effect of Temperature on the Performance of a Silicon Heterojunction Solar Cell (HIT) in the Presence of Excitons. *International Journal of Materials Science and Applications, Special Issue : Advanced Materials for Energy Storage and Conversion Applications*, Vol. 8, N°4, pp 56-67.
- [12]. Amoupour, E., Abdolazadeh Ziabari, A., Andarva, H., & Ghodsi, F. E. (2014). Influence of air/N<sub>2</sub> treatment on the structural, morphological and optoelectronic traits of nanostructured ZnO:Mn thin films. *Superlattices and Microstructures*, 65, 332–343.
- [13]. A. B. khatibani, A. A. Ziabari, S. M. Rozati, Z. Bargbidi, and G. Kiriakidis. Characterization and Gas-sensing Performance of Spray Pyrolysed In<sub>2</sub>O<sub>3</sub> Thin Films: Substrate Temperature Effect. *Transactions on Electrical and Electronic Materials*, vol. 13, no. 3, pp. 111–115, Jun. 2012.
- [14]. Hiroshi Yanagi, Hiroshi Kawazoe, Atsushi Kudo, Masahiro Yasukawa and Hideo Hosono. Chemical Design and Thin Film Preparation of p-Type Conductive Transparent Oxides. *Journal of Electroceramics* 4 (2/3), 407-414, 2000.
- [15]. Xiliang Nie, Su-Hai Wei, and S. B. Zhang. Bipolar Doping and Band-Gap Anomalies in Delafossite Transparent Conductive Oxides. *Physical Review Letters* 88 (6), 066405(1-4), 2002.

- [16]. Yu Yang, Shu Jin, Julia E. Medvedeva, John R. Ireland, Andrew W. Metz, Jun Ni, Mark C. Hersam, Arthur J. Freeman, and Tobin J. Marks. *Journal American Chemical Society* 127 (24), 8796-8804, 2005.
- [17]. Leonard Tutsch, Frank Feldmann, Bart Macco, Martin Bivour, Erwin Kessels, and Martin Hermle. Improved Passivation of n-Type Poly-Si Based Passivating Contacts by the Application of Hydrogen-Rich Transparent Conductive Oxides. *IEEE Journal of Photovoltaics* 10 (4), 986-991, 2020.
- [18]. Takashi Koida, Hiroyuki Fujiwara, and Michio Kondo. Hydrogen-doped  $\text{In}_2\text{O}_3$  as high-mobility transparent conductive oxide, *Japanese Journal of Applied Physics* 46 (28), 685-687, 2007.
- [19]. D. Gaspar, L. Pereira, K. Gehrke, B. Galler, E. Fortunato, R. Martins. *Solar Energy Materials & Solar Cells* 163, 255-262, 2017.
- [20]. Takashi Koida, Hiroyuki Fujiwara, and Michio Kondo. Structural and electrical properties of hydrogen-doped  $\text{In}_2\text{O}_3$  films fabricated by solid-phase crystallization. *Journal of Non-Crystalline Solids* 354 (19), 2805-2808, 2008.
- [21]. Barraud L, Holman ZC, Badel N, Reiss P, Descoedres A, Battaglia C, De Wolf S, Ballif C. Hydrogen-doped indium oxide/indium tin oxide bilayers for high-efficiency silicon heterojunction solar cells. *Solar Energy Materials and Solar Cells* 115, 151-156, 2013.
- [22]. Wardenga HF, Frischbier MV, Morales-Masis M, Klein A. In Situ Hall Effect Monitoring of Vacuum Annealing of  $\text{In}_2\text{O}_3$  : H Thin Films. *Materials* 8(2), 561-574, 2013.
- [23]. Yuqiang Liu, Yajuan Li, Yiliang Wu, Guangtao Yang, Luana Mazzarella, Paul Procel-Moya, Adele C. Tamboli, Klaus Weber, Mathieu Boccard, Olindo Isabella, Xinbo Yang and Baoquan Sun. High-Efficiency Silicon Heterojunction Solar Cells: Materials, Devices and Applications. *Materials Science & Engineering R* 142, 1-116, 2020.
- [24]. Takashi Koida, Hiroyuki Fujiwara, and Michio Kondo. High-mobility hydrogen-doped  $\text{In}_2\text{O}_3$  transparent conductive oxide for a-Si:H/c-Si heterojunction solar cells. *Solar Energy Materials and Solar Cells* 93(6), 851-854, 2009.
- [25]. L. Barraud, Z.C. Holman, N. Badel, P. Reiss, A. Descoedres, C. Battaglia, S. De Wolf, C. Ballif. **Hydrogen-doped indium oxide/indium tin oxide bilayers for high-efficiency silicon heterojunction solar cells.** *Solar Energy Materials and Solar Cells* 115, 151-156, 2013.
- [26]. Timo Jäger, Yaroslav E. Romanyuk, Shiro Nishiwaki, Benjamin Bissig, Fabian Pianezzi, Peter Fuchs, Christina Gretener, Max Döbeli, and Ayodhya N. Tiwari. Hydrogenated indium oxide window layers for high-efficiency  $\text{Cu}(\text{In,Ga})\text{Se}_2$  solar cells. *Journal of Applied Physics* 117 (20), 5301(1-7), 2015.

- [27]. Fan Fu, Thomas Feurer, Timo Jäger, Enrico Avancini, Benjamin Bissig, Songhak Yoon, Stephan Buecheler and Ayodhya N. Tiwari. Low-temperature-processed efficient semi-transparent planar perovskite solar cells for bifacial and tandem applications 18 (6), 8932(1-9), 2015.
- [28]. Rebert W. Miles, Kathleen M. Hynes and Ian Forbes. Photovoltaic solar cells : An overview of state-of-the-art cell development and environmental issues. *Progress in Crystal Growth and Characterization of Materials* 51 (1-3), 1-42, 2005.
- [29]. Martin A. Green. Intrinsic concentration, effective densities of states, and effective mass in silicon. *Journal of Applied Physics* 67 (6), 2944-2954, 1990.
- [30]. Rudi C. Vankemmel, Wim Schoenmaker and Kristin M. de Meyer. A unified wide temperature range model for the energy gap, the effective carrier mass and intrinsic concentration in silicon. *Solid-State Electronics* 36 (10), 1379-1384, 1993.
- [31]. Yatendra Pal Varshni. Temperature dependence of the energy gap in semiconductors. *Physica* 34 (1), 149-154, 1967.
- [32]. C. D. Thurmond. The Standard Thermodynamic Functions for the Formation of Electrons and Holes in Ge, Si, GaAs, and GaP. *Journal of The Electrochemical Society* 122 (8), 1133-1141, 1975.
- [33]. V. Alex, S. Finkbeiner and J. Weber. Temperature dependence of the indirect energy gap in crystalline silicon. *Journal of Applied Physics* 79 (9), 6943-6946, 1996.
- [34]. A. Sproul et M. Green. Improved value for the silicon from 275 to 375 K. *Journal of Applied Physics* 70 (2), 846-854, 1991.
- [35]. P. Norton, T. Braggins and H. Levinstein. Impurity and Lattice Scattering Parameters as Determined from Hall and Mobility Analysis in n-Type Silicon. *Physical Review* 8 (12), p. 5632-5653, 1973.
- [36]. C. Canali, C. Jacoboni, G. Ottaviani, and A. Alberigi-Quaranta. High-field diffusion of electrons in silicon. *Quaranta Applied Physics Letters* 27 (5), 278-280, 1975.
- [37]. Carlo. Jacoboni, Claudio. Canali, Giampiero P. Ottaviani et Alessandro Alberigi-Quaranta. A review of some charge transport properties of silicon. *Solid-State Electronics* 20 (2), 77-89, 1977.
- [38]. Shengsan Li and Rebert W. Thurber. The dopant density and temperature dependence of electron mobility and resistivity in n-type silicon. *Solid-State Electronics* 20 (7), 609-616, 1977.
- [39]. G. Masetti, M. Severi and S. Solmi. Modeling of carrier mobility against carrier concentration in arsenic-, phosphorus-, and boron-doped silicon. *IEEE Transactions on Electron Devices* 30 (7), 764-769, 1983.
- [40]. Dirk B. M. Klaassen. A unified mobility model for device simulation-I. model equations and concentration dependence. *Solid-State Electronics* 35 (7), 953-959, 1992.
- [41]. Dirk B. M. Klaassen. A unified mobility model for device simulation-II. Temperature dependence of carrier mobility and lifetime. *Solid-State Electronics* 35 (7), 961-967, 1992.